Yale University
EliScholar – A Digital Platform for Scholarly Publishing at Yale

Yale Medicine Thesis Digital Library | School of Medicine

9-27-2010

Incidence of Leukoencephalopathies With Restricted Diffusion On Magnetic Resonance Imaging

Michael William DeStefano
Yale University

Follow this and additional works at: http://elischolar.library.yale.edu/ymtdl

Recommended Citation
DeStefano, Michael William, "Incidence of Leukoencephalopathies With Restricted Diffusion On Magnetic Resonance Imaging" (2010). *Yale Medicine Thesis Digital Library*. 203.
http://elischolar.library.yale.edu/ymtdl/203

This Open Access Thesis is brought to you for free and open access by the School of Medicine at EliScholar – A Digital Platform for Scholarly Publishing at Yale. It has been accepted for inclusion in Yale Medicine Thesis Digital Library by an authorized administrator of EliScholar – A Digital Platform for Scholarly Publishing at Yale. For more information, please contact elischolar@yale.edu.

Incidence of Leukoencephalopathies With Restricted Diffusion On Magnetic Resonance Imaging

A Thesis Submitted to the
Yale University School of Medicine
In Partial Fulfillment of the Requirements for the
Degree of Doctor of Medicine

By
Michael William DeStefano
2010

ABSTRACT

INCIDENCE OF LEUKOENCEPHALOPATHIES WITH RESTRICTED DIFFUSION ON MAGNETIC RESONANCE IMAGING.

Michael W. DeStefano, Joachim M. Baehring, and Robert K. Fulbright. Department of Diagnostic Radiology, Yale University, School of Medicine, New Haven, CT.

The purpose of our study was to determine the incidence, causes, and reversibility of leukoencephalopathies demonstrating confluent areas of restricted diffusion on magnetic resonant imaging (DWI+LE). We hypothesized DWI+LE would have a low incidence, and be primarily caused by toxic exposures. We performed a logic sentence based search of the Yale-New Haven MRI database to select for reports indicating restricted diffusion within the cerebral white matter. We examined patients' neuroimaging studies and medical record. We identified a total of 35 cases of DWI+LE, which resulted in an overall incidence of 0.2% over the five-year period queried. The medical conditions associated with DWI+LE were as follows: toxic exposure (7), hypoxia with concurrent trauma (7), hypoxia with concurrent toxic exposure (4), hypoxia with concurrent metabolic derangements (4), seizure with concurrent metabolic derangements (2), metabolic derangements (2), antiepileptic therapy (2), hypoxia (1), trauma (1), and unknown (5). The most favorable outcomes were seen in patients with intrathecal methotrexate toxicity, while patients with hypoxia without a lucid interval fared worst. We concluded that DWI+ LE are rare, their etiology diverse, and its reversibility dependant upon the type and severity of the insult.

ACKNOWLEDGMENTS

I would like to thank my parents, sisters, and friends. Their love and support sustained me throughout medical school. I would also like to thank my research advisors, Dr. Fulbright and Dr. Baehring, for their guidance. I would like to acknowledge the office of student research for the short-term research funding I received.

TABLE OF CONTENTS

ABSTRACT: 2

ACKNOWLEDGMENTS: 3

INTRODUCTION: 5-15

HYPOTHESIS AND OBJECTIVES: 16

METHODS: 17

RESULTS: 18-22

DISCUSSION: 23-26

CONCLUSIONS: 27

FIGURES: 28-29

TABLES: 30-35

REFERENCES: 36-38

INTRODUCTION

Nuclear Magnetic Resonance

Nuclear magnetic resonance (NMR) is a property of magnetic nuclei first described in 1938 by Isidor Isaac Rabi in a molecular beam of LiCl.[1] Edward Purcell and Felix Bloch expanded upon Rabi's work for use in solids and liquids. They discovered that when magnetic nuclei are placed in a magnetic field and subjected to a pulse of electromagnetic energy, they radiate energy back out at a specific "resonant" frequency that depended on the composition of the nucleus and strength of the applied magnetic field. Over 30 years later, Paul Lauterbur published the first method of using NMR to create an image.[2] Lauterbur created a two-dimensional image of capillary tubes of H_2O submerged in D_2O. At that time, no other imaging technique could distinguish between the two different types of water. The genius behind Lauterbur's experiment was the use a magnetic field gradient in order to localize the position of the resonant nuclei emitting energy. This concept allowed NMR to generate an image, and proved revolutionary.

NMR imaging developed throughout the 1970's with the first image of a human subject published in 1977.[3] Subsequently, NMR imaging became known as simply magnetic resonance imaging (MRI) due to the negative, societal connotations associated with the word "nuclear". Since MRI depends solely upon the application of a magnetic field and radiofrequency energy, this negative connotation is wholly undeserved. MRI allows for the visualization of internal tissue structures without any exposure to harmful ionizing radiation.

In order to understand NMR, it is necessary to comprehend the interaction between a magnetic nucleus and an external magnetic field. NMR relies upon the

property of an atom's nucleus known as spin. The nucleus of an atom contains two types of fundamental particles, protons that are positively charged, and neutrons that have no charge. Both protons and neutrons possess an intrinsic motion known as spin. Although it is tempting to imagine spin as the product of smaller constituents rotating around a center of mass, neutrons and protons are elementary particles that cannot be further divided. Therefore, it is better to conceptualize spin like other intrinsic properties of elementary particles such as resting mass or charge.

In order for a nucleus to be considered magnetic, it must have a net spin. This makes intuitive sense since a moving electrical charge induces a magnetic field. Further, quantum mechanics requires the nuclear spin value be discrete and quantized. The spin value must be zero, an integer, or half-integer. Since the spins of two protons or two neutrons cancel each other out, nuclei with an even number of protons and neutrons, such as ^{16}O, have a zero spin. An integer spin value is found in nuclei with an odd number of protons and/or neutrons, such as ^{2}H. A half-integer spin value is found in nuclei with an even number of neutrons and odd number of protons or vice-versa, such as ^{13}C.

A beaker of pure H_2O will contain billions of magnetic nuclei in the form of ^{1}H, but as a whole will have no net magnetization. Since the nuclei are spinning in random orientations, their magnetic fields have the net effect of canceling each other out. This is why NMR requires not only magnetic nuclei, but also the application of a magnetic field.

When placed in an external magnetic field, magnetic nuclei align themselves with the applied field. They can align themselves into two different states. One state is high-energy and anti-parallel to the direction of the external magnetic field, while the other is low-energy and parallel to the external magnetic field. Any given nucleus is capable of

switching between alignments, but there is a slight overall preference for the low-energy state. On aggregate, this creates a net magnetization. Stronger applied magnetic fields increase the amount of energy needed to switch between states, resulting in more nuclei remaining in the parallel state, and increasing the net magnetization.

Thermal energy prevents spinning in direct vertical alignment with the external magnetic field. The magnetic nucleus is pushed into a rotation around an axis of the applied field. This rotation is known as precession, and the rate of precession is related to the magnetic field strength and composition of the nucleus. This relationship is key to MRI and is known as the Larmor frequency.

$$\omega_o = \gamma B_o /2\pi$$

Where, ω_o is the Larmor frequency, B_o is the magnetic field strength, and γ is the gyromagnetic ratio, a constant for specific to each nucleus. If energy is applied at the Larmor frequency, the spin can absorb this energy and move from a low-energy to high-energy state through a process known as resonance absorption. This is why the Larmor frequency is also known as the resonance frequency.[4]

Now that we have explored the properties of magnetic nuclei placed in an external magnetic field, we can approach how this is used to create an image. Since ^1H is abundant in the form of water within the human body, it is the most commonly imaged nucleus in MRI. For the sake of simplicity, I will refer to its imaging from this point forward.

Images are acquired by placing the patient into a strong homogeneous magnetic field. As discussed above, this aligns the magnetic hydrogen nuclei within the patient's body with the external magnetic field. The slight preference for the parallel state creates a

net magnetization in the direction of the external magnetic field, known as longitudinal magnetization. Next, a radiofrequency pulse oscillating precisely at the Larmor frequency is applied. The hydrogen nuclei absorb this energy causing the net magnetization to rotate away from the longitudinal orientation into a perpendicular, transverse plane. If the radiofrequency pulse is applied for long enough and in the right direction, the entire longitudinal magnetization will rotate into the transverse plane, and is known as 90-degree pulse.

When the radiofrequency pulse is turned off, the hydrogen nuclei's spins will return to their original orientation and emit energy at the same Larmor frequency. This process is known as relaxation, and creates a voltage in the transverse plane. The voltage decays at a rate dependent upon the relaxation of the hydrogen proton spins, and is measured by a loop of wire. This voltage is the basis of the MR signal.

Two different types of changes occur when the radiofrequency pulse is turned off. Spin dispersion in the transverse plane and spin realignment back into the longitudinal plane. Proton spin dispersion results in an irreversible decrease in the transverse magnetization, and is known as T2 relaxation. The T2 relaxation time is defined as the time required for the transverse component of the magnetic field to return to 37% of its value following excitation. T2 relaxation results from small differences in the precession rates of the excited hydrogen protons due to local inhomogeneity in the magnetic field. Since T2 relaxation is the result of interactions between the excited spins, it is also known as spin-spin relaxation.[4]

Spin realignment into the longitudinal plane is known as T1 relaxation. The T1 relaxation time is defined as the time required for the longitudinal component of the

magnetic field to return to 63% of its initial value. T1 relaxation is the result of hydrogen proton spins losing energy to the surrounding environment, and seeking a lower energy state. Since T1 is the result of interactions between the spins and the environment, it is also known as spin-lattice relaxation.[4]

Both types of change in spin cause voltage decay that can be measured by a receiver coil. The amount of time you allow to elapse between excitation and detection by the receiver coil determines whether T1 or T2 relaxation generates the signal measured. Spins in different microenvironments have different T1 and T2 relaxation rates, allowing for image contrast. For example, cerebrospinal fluid is dark on T1-weighted images, while fat is bright. Alternatively, cerebrospinal fluid is bright on T2-weighted images, while fat has an intermediate signal intensity.[5]

Spatial encoding in MR imaging uses magnetic field gradients. The intensity of the magnetic field varies linearly along the gradient application axis. These magnetic field gradients are characterized by amplitude, direction, duration and moment of application. These gradients allow the encoding of spatial data as spatial frequency information. These data are mapped into k-space so that an inverse two-dimensional Fourier transformation reconstructs the MR image.

The slice selection gradient modifies the precession frequency of the protons so that a radiofrequency wave of the same frequency will cause them to shift. The selective pulse bandwidth and gradient amplitude will determine the slice thickness. The slice selection gradient is simultaneously applied to all the radiofrequency pulses. The phase encoding gradient differentiates the rows of k-space. The phase encoding gradient is regularly incremented, as many times as there are rows to receive, leading to different

phase shifts for each voxel line. The frequency encoding gradient differentiates the columns. Its application gives distinct frequencies to each voxel column. In three-dimensional imaging, more phase encoding steps are applied in the third spatial direction. This lengthens acquisition time, but three-dimensional imaging improves spatial resolution and the signal to noise ratio.

Phase and frequency encoding can be compared to a sieve or filter that is sensitive to spatial distribution in the horizontal and vertical directions. The gradient value determines how fine a sieve or filter is. The entire set of data is combined in the radiofrequency signal simultaneously received on applying the frequency encoding gradient. All the signals of the same slice are recorded in a matrix, and then processed to form an image of the slice plane.

The location of the data in k-space depends on the strength and the duration of the gradients. If no gradient is applied, the location is at the center of k-space. The higher the net strength of the gradient, or the longer the gradient is applied, the farther from the origin of k-space the data will be located. Gradients are bipolar (negative or positive), so it is possible to move in opposite directions from the center (to the left or the right, and to the top or the bottom).

Each point of k-space encodes for spatial information of the entire MR image. Therefore, each point of the MR image is the result of the combination of all the data of k-space. The data along a line passing through the center of k-space represent the Fourier transformation of the projection of the image onto a line with the same orientation. A point in k-space encodes for image signal variations in the same direction as the line passing through this point and the center of k-space.

The center of k-space contains low-spatial-frequency information. Most image information is contained in low-spatial-frequency information, corresponding to general shape and contrast. The periphery of k-space does not correspond to periphery of the image. It contains high-spatial-frequency information. The higher the spatial frequency, the smaller are the details of the image.

Diffusion Weighted Imaging Background

Diffusion weighting imaging (DWI) is a modification of regular MRI techniques first utilized in 1984 by Michael Moseley. DWI detects variations in the thermal diffusion of water molecules, also known as Brownian motion. First, a pulsed field gradient is used to cause the homongeneity of the magnetic field to vary linearly. Since precession is related to magnetic field strength, the protons begin to precess at different rates. This causes dispersion of phase between spins, and therefore signal loss. Another gradient pulse is applied in the same direction but with an opposite magnitude. This refocuses the spins, but will not be as successful for spins that have moved during the time interval between pulses. The following equation relates the decrease in signal due to the application of the two pulse gradients to the amount of thermal diffusion:

$$S = S_0 e^{(-bADC)}$$

Where S is the signal with the gradient, S_0 is the signal without the gradient, ADC is the apparent diffusion coefficient, and b is the gradient factor.

From this equation, we can see that tissues with a higher ADC value will produce lower signal intensity. Since cerebrospinal fluid contains water that is relatively free to engage in thermal diffusion, its ADC is high, and results in a low signal on DWI. An area

of higher signal intensity on DWI indicates cellular membranes and tissue constituents are restricting water's diffusion.[6]

DWI has an associated T2-weighted component. With two acquisitions at different b-factors (typically b = 0 and 1000 s/mm2), it is possible to calculate the ADC to remove the T2 part. This is useful in cases when a T2 hypersignal appears as a hypersignal on DWI, and allows for the differentiation between T2-shine-through and true restricted diffusion.

DWI provides us with valuable information about underlying brain structure and function. In 1990, Moseley published a study using cats that demonstrated DWI could identify the effects of acute stroke better than conventional MRI and computed tomography. This quickly led to an explosion of interest in DWI. Almost all MRI scans of the brain now include sequencing for DWI. It is routinely used in the early detection of ischemic stroke, identifying active plaques in multiple sclerosis, differentiating arachnoid cyst from epidermoid tumor, and distinguishing brain abscess from neoplasm.[7, 8]

DWI is also able to differentiate between vasogenic and cytotoxic edema. The former is characterized by an excess of extracellular water from either leaky blood vessels or the break down of the blood-brain barrier, and results in relatively low signal on DWI. On the other hand, cytotoxic edema reflects the inability of the cells to maintain water balance between the extracellular and intracellular spaces, and results in high signal intensity on DWI.[9] It is precisely DWI's ability to provide information regarding water's thermal movement at the cellular level that has made it an indispensable tool for clinical management, as well as, investigating the molecular pathophysiology behind diseases.

Leukoencephalopathy and Restricted Diffusion

Structural alterations that predominantly affect the cerebral white matter are known as leukoencephalopathies. The clinical manifestations of white matter damage are highly variable, but the most distinctive presentation is a change in mental status with the preservation of language.[10] Leukoencephalopathy is the common result of toxin exposure, inflammation, infection, metabolic insult, cerebrovascular disease, trauma, and hydrocephalus. Leukoencephalopathies that demonstrated confluent areas of restricted diffusion (DWI+LE) are rare, and a literature review reveals primarily case reports.

Toxic exposure is the mostly widely reported cause of DWI+LE. Methotrexate, 5-fluorouracil, carmofur, capecitabine and inhalation of heroin have all been implicated in DWI+LE.[11-15] The mechanism by which toxins lead to restricted water diffusion in the cerebral white matter remains under investigation, but since the lesions do not correspond to vascular territories, a vasculopathic etiology is unlikely. Animal studies using 5-fluorouracil and human autopsy reports from heroin abusers reveal vacuolation with splitting of the myelin intraperiod line.[16-18] Conceivably, fluid entrapment between the myelin lamellae causes the restricted water diffusion seen on DWI, but it is unclear whether this will represent a unifying neuropathological correlate.

Typically, hypoxic injury causes a greater insult to gray matter structures due to their higher energy demands. A rare condition reported in the literature is a post-hypoxic DWI+LE. Clinical manifestations and imaging abnormalities can be delayed days to weeks from the time of insult. The incidence of post-hypoxic DWI+LE has been reported to range from 1-28 per 1,000 patients who suffer a hypoxic event, and may be associated with carbon monoxide poisoning. The injury is usually reversible with the majority of

cases reporting a remarkable clinical recovery. The pathogenesis behind this DWI+LE is poorly understood, but may be related to programmed cell death of oligodendrocytes.[19, 20]

Metabolic abnormalities such as hypoglycemia, hyponatremia, and acute exacerbations of phenylketonuria and maple syrup urine disease have been reported to cause DWI+LE. In maple syrup urine disease, branched chained amino acids can accumulate to toxic levels within the cerebral white matter. Similarly, phenylketonuria results in the toxic build up of phenylalanine. Both are extremely rare genetic conditions occurring in approximately 1 in 180,000 births for maple syrup urine disease, and 1 in 15,000 births for phenylketonuria. It is important to note that the incidence of these diseases can vary dramatically between different human populations, and consequently, the incidence of DWI+LE from acute exacerbations would be expected to greatly vary. Recent reports used diffusion tensor imaging (DTI), a modification of DWI that evaluates changes in anisotropic diffusion, to suggest these two DWI+LE are the result of reversible intramyelinic sheath edema. A reversible decrease in the fractional anisotropy implicates swelling of the myelin sheath. This accumulation of fluid would allow increased thermal diffusion in all directions, decreasing the preference for diffusion along the directions parallel to the nerve fibers. [21-23]

Numerous cases reports have also implicated antiepileptic drugs in DWI+LE. Almost universally, the corpus callosum is the only structure involved. It is postulated that antiepileptic drugs' influence on the arginine-vasopressin fluid balance system is responsible for the restricted water diffusion.[24, 25] DTI has also been used to suggest these DWI+LE are the result of reversible intramyelinic sheath edema.[26]

Finally, trauma commonly results in injury to the cerebral white matter. Shearing forces from the rapid acceleration and deceleration experienced in motor vehicle accidents, shaking trauma, and falls sever axons. Traumatic white matter injury is most often seen scattered along the gray-white junction, but trauma can also result in confluent areas of white matter injury. DWI+LE following trauma typically occurs in the corpus callosum, dorsal aspect of the upper brain stem, and the white matter of the frontal and temporal lobes.[6]

HYPOTHESIS AND OBJECTIVES

The primary objective of our study was to determine the incidence of DWI+LE in a single institutional cohort. We also aimed to characterize the various causes of this syndrome, and determine their reversibility. DWI+LE incidence data are important in order to establish its probability in patients presenting with neurologic symptoms that are consistent with white matter damage. Proper, timely diagnosis is essential for treatment. Epidemiological data will also allow for clinicians to generate a reasonable differential upon imaging confirmation of DWI+LE. We hypothesized that the incidence of DWI+LE would be low with toxic exposure representing the primary etiology.

METHODS

We performed a retrospective, logic sentence based search of the Yale-New Haven MRI database from September 2003 to September 2008 in order to select for reports that indicated confluent areas of reduced water diffusion within the cerebral white matter. We reviewed the patients' pertinent neuroimaging studies and the medical record. All DWI abnormalities were confirmed with an apparent diffusion coefficient map.

The logic sentence used for the search was as follows: slow diffusion or restricted diffusion and (white matter or leukoencephalopathy or acute ischemia or chemotherapy or methotrexate or hypoxia or hypoglycemia or drug overdose or heroin or metabolic).

Cases of cellular neoplasms, acute cerebrovascular accident, and abscess were carefully excluded. It is also important to note that our inclusion criteria emphasized that the areas of restricted diffusion be confluent. This criterion lead to the exclusion of cases of diffuse axonal injury scattered along the gray-white junction as well as cases of multiple sclerosis, in which restricted diffusion is often seen along the rim of active plaques.

RESULTS

From a total MRI scan volume of 17,420 unique patients, we identified 35 cases of DWI+ LE fulfilling the inclusion criteria. This resulted in an incidence of 0.2% over the five-year period queried. 20 patients were male, and 15 patients were female. The median age was 19.

The relative contribution by etiology was as followed: 20% toxin exposure, 20% hypoxia with concurrent trauma, 11% hypoxia with concurrent metabolic derangements, 11% toxin exposure with concurrent hypoxia, 6% metabolic derangements alone, 6% seizure with concurrent metabolic derangements, 6% antiepileptic therapy, 3% hypoxia alone, 3% trauma alone, and 14% unknown.

TOXIC EXPOSURE

In seven cases, toxic exposure preceded DWI+ LE. Three cases followed intrathecal methotrexate administration for leukemia. One involved the bilateral corona radiata and cortical spinal tracts, another involved the left frontoparietal white matter (Figure 1), and the last involved the bilateral frontoparietal white matter. All three of these patients showed complete symptom and imaging resolution. One case followed intravenous methotrexate administration for lymphoma, involved the right corona radiata, and resulted in complete symptom resolution. One case followed salicylate ingestion, involved the bilateral periventricular white matter, and resulted in complete symptom resolution. One case followed heroin abuse, involved the white matter of all the lobes of the cerebral hemispheres and corpus callosum, and resulted in a complete clinical recovery. Finally, one case followed crack-cocaine abuse, involved the bilateral

periventricular white matter and left cerebellum, and resulted in death eight days following admission with no clinical improvement. More detailed data on the clinical presentation, imaging findings, and outcomes of these patients can be found in Table A.

TRAUMA/HYPOXIA

In seven cases, trauma with concurrent hypoxia preceded DWI+ LE. Three cases followed motor vehicle accidents (one involved the corpus callosum, left anterior temporal white matter, and left corona radiata, one involved the bilateral frontal white matter, deep left parietal white matter and the corpus callosum, and one involved the centrum semiovale, periventricular white matter and the corpus callosum). All three of these patients showed significant clinical improvement. Two cases followed non-accidental shaking trauma (one involved the corpus callosum and bilateral optic radiations, and showed partial imaging resolution four months later, the other involved the left cerebral white matter and right inferior frontal white matter, and made a partial clinical recovery). Two cases followed intracranial bleeds. Both involved the entire corpus callosum. One of these made a full clinical recovery while follow-up data on the other is unknown. More detailed data on the clinical presentation, imaging findings, and outcomes of these patients can be found in Table B.

TOXIC/HYPOXIA

In four cases, toxin exposure with concurrent hypoxia preceded DWI+LE. One case followed severe respiratory depression with cocaine/opiate abuse, and involved the bilateral cerebral and cerebellar hemispheres as well as the corpus callosum. This patient

made a partial clinical recovery. One case followed a pulseless electrical activity with methadone/cocaine abuse, involved the bilateral parietal periventricular white matter, and resulted in a partial clinical recovery. One case followed pulseless electrical activity with benzodiazepine/cocaine abuse, involved the bilateral posterior limbs of the internal capsule, and resulted in death two days after admission. One case followed respiratory arrest with benzodiazepine/cocaine/opiate abuse, and involved the bilateral periventricular and subcortical white matter (Figure 2). This patient made a full clinical recovery with complete imaging resolution. More detailed data on the clinical presentation, imaging findings, and outcomes of these patients can be found in Table C.

HYPOXIA/METABOLIC

In four cases, neonatal hypoxia with concurrent metabolic abnormalities preceded DWI+ LE. One case followed hyponatremia/kalemia/hypocalcemia and elevated liver enzymes, and involved the bilateral periventricular white matter. One case followed hyperkalemia/hyponatemia and elevated direct bilirubin, and involved the bilateral posterior periventricular white matter. One case followed hypocalcemia and elevated direct bilirubin, and involved the bilateral periventricular white matter. One case followed hypochloremia/kalemia and elevated liver enzymes, and involved the bilateral subcortical frontal, parietal and occipital white matter. Clinical and imaging follow-up is unknown for all four of these patients. More detailed data on the clinical presentation, and imaging findings of these patients can be found in Table D.

METABOLIC

In two cases, metabolic abnormalities alone preceded DWI+LE. One case followed rapidly corrected hyponatremia, and involved the central midbrain. One case followed hypoglycemia, involved the splenium of the corpus callosum (Figure 3), and resulted in complete clinical and imaging resolution. More detailed data on the clinical presentation, imaging findings, and outcomes of these patients can be found in Table E.

SEIZURE/METABOLIC

In two cases, metabolic derangements with concurrent seizure preceded DWI+LE. One case followed seizure with hypocalcemia and dehydration, and involved the bilateral occipital and temporal white matter. One case followed seizure with hyponatremia/kalemia, involved the posterior corpus callosum, and showed imaging resolution. More detailed data on the clinical presentation, imaging findings, and outcomes of these patients can be found in Table F.

ANTIEPILEPTICS

In two cases, antiepileptic therapy was thought be of pathogenic relevance to the DWI+LE. One case followed the administration of valproic acid and oxcarbazepine, and the other followed the administration of lamotrigine, oxcarbazepine, and topiramate (Figure 4). Both cases involved the splenium of the corpus callosum, and follow-up data are unknown. More detailed data on these patients can be found in Table G.

HYPOXIA

In one case, a hypoxic event alone preceded DWI+ LE. The patient experienced pulseless electrical activity secondary to aspiration, and imaging showed confluent areas of restricted diffusion throughout the white matter. The patient died 19 days later. More detailed data on this patient can be found in Table H.

TRAUMA

In one patient, trauma alone preceded DWI+LE. The patient experienced head trauma in a go-cart accident, and imaging showed restricted diffusion in the splenium of the corpus callosum. Follow-up is data unknown. More detailed data on this patient can be found in Table I.

UNKNOWN ETIOLOGY

In five cases, the etiology of DWI+LE remains unknown despite extensive work-up. More detailed data on the clinical presentation, imaging findings, and outcomes of these patients can be found in Table J.

DISCUSSION

DWI+LE incidence data are imperative in order to ascertain its likelihood in patients presenting with neurologic symptoms that are consistent with white matter damage. This data will guide timely diagnosis and proper treatment. Epidemiological data will also allow clinicians to generate a reasonable differential upon imaging confirmation of DWI+LE.

Epidemiological data of DWI+LE is scare. Best estimates indicate it occurs in less than 2 % of recipients of methotrexate.[27] We found DWI+ LE in 0.2% of patients receiving brain MRIs over a five-year period at our institution. Given the paucity of epidemiological data regarding DWI+LE, our study significantly contributes to the existing literature, and identifies the contribution of the various medical conditions, with which it is associated. Case ascertainment in our study was likely incomplete based on its retrospective design, and its reliance on a logic sentence based search.

DWI+LE have been associated with a variety of toxin exposures and metabolic derangements. It occurs after intrathecal as well as intermediate to high dose intravenous methotrexate administration, 5-fluorouracil, carmofur or capecitabine. Other causes of DWI+LE identified in our case series and reported by others are illicit and therapeutic drug use, carbon monoxide poisoning, hypoxia, hypoglycemia, hyponatremia, seizure, antiepileptic drug therapy, trauma, high altitudes, acute exacerbations of maple syrup urine disease, and phenylketonuria.

Toxin exposure was the most common single etiology leading to DWI+LE in our cases series. We identified DWI+LE following intrathecal and intravenous administration of methotrexate, heroin use, crack use, and aspirin overdose. The

presenting symptoms often mimicked that of a cerebral vascular accident. This can poses a particularly challenging clinical problem for patients receiving chemotherapy for malignant neoplasm since their hypercoagulable state places them at increased risk for stroke. The correct diagnosis is essential for proper treatment. DWI+LE should be included in the differential of any patient receiving these chemotherapeutic agents, and presenting with stroke-like symptoms.

The injury in toxic DWI+LE can be readily reversible. In our case series, six of the seven patients with a purely toxic etiology showed complete resolution of their symptoms, and all three patients who received imaging follow-up showed DWI signal normalization. Clinical and radiologic reversibility is strongly supported by others in the literature.[11, 12]

In our case series, DWI+LE followed hypoxic-ischemic events in 15 patients, but all had additional contributing factors. We found DWI+LE following a hypoxic-ischemic event with concurrent head trauma in seven patients, concurrent metabolic abnormalities in four neonatal patients, concurrent illicit drug abuse in three patients, and a demyelinating disease in remission in one patient. The role toxins, metabolic abnormalities, head trauma, and prior white matter injury may play in preferentially sensitizing white matter to hypoxic injury remains speculatory, but some have suggested an association between post-hypoxic DWI+LE and a pseudodeficiency of arylsulfatase A.[20] Further, DWI+LE following neonatal hypoxia has been associated with decreased brain maturity, and results in better clinical outcomes than infants with hypoxic gray matter damage.[28] In our series, adults with hypoxic injury who did not experience a lucid interval fared worst. Half of these patients died within a month of admission.

We identified one case of hypoglycemia leading to DWI+LE that involved solely the corpus callosum. Hypoglycemia usually affects the cortex, but cases of DWI+LE following hypoglycemia have been reported by others, and is hypothesized to result from the release of excitatory amino acids into the extracellular space.[29, 30] The other metabolic cause of DWI+LE identified in our series involved the central midbrain, and was due to rapidly corrected hyponatremia. This phenomenon is known as central pontine myelinolysis. The osmolar disturbance created by a rapid change in serum sodium concentration causes destruction of the myelin sheaths by a still ill defined mechanism. DWI has also been shown to detect central pontine myelinolysis earlier than conventional MRI techniques.[31] We did not identify any cases of DWI+LE following acute exacerbations of maple syrup urine disease or phenylketonuria, but this is not surprising since both are exceedingly rare pediatric conditions.

We identified DWI+LE following a first time seizure in two patients, both of whom had concurrent metabolic derangements. The development of DWI+LE following seizure is unexpected since the foci of seizure activity are cortical neurons. DWI+LE localized to the splenium of the corpus callosum following seizure has been postulated to represent transient edema related to transhemispheric transmission of secondary generalized seizure activity.[32]

We also identified DWI+LE in two patients who had been on multiple combinations of antiepileptic drug therapy. One was admitted on oxcarbazepine and valproic acid, and the other was admitted on oxcarbazepine, lamotrigine, and topiramate. Both patients had DWI+LE confined to the corpus callosum, which is consistent with the reports in the literature.[24-26] Whether or not this represented reversible intramyelinic

sheath edema, as postulated by others, is unknown since we do not have follow-up imaging data on these two patients.

Trauma alone led to DWI+LE in one patient in our series. Our inclusion criteria emphasized that the areas of restricted diffusion be confluent and contained within the white matter. This led to the exclusion of patients with axonal injury scattered along the gray-white junction, which is the most common site of involvement in traumatic brain injury. As previously mentioned, we identified seven cases of DWI+LE following trauma with concurrent hypoxic injury. This is not surprising since trauma often results in respiratory arrest and/or cardiovascular collapse. Subarachnoid hemorrhage can also lead to hypoxic-ischemic injury by inducing vasospasm. DWI+LE observed in traumatic brain injury is thought to result from the development of retraction balls and concomitant cytoskeletal collapse along the severed axons as well as cellular swelling and intramyelinic edema from excitiotoxic mechanisms that propagate along the white matter tracts.[33, 34] This cytotoxic and intramyelinic edema has been shown to be potentially reversible.[35] The outcomes observed in our series support the notion of reversibility with clinical and/or radiologic improvement seen almost universally.

CONCLUSIONS

DWI+ LE are rare and their etiology diverse. We found an overall incidence of 0.2% over the five-year period queried. Shared radiographic characteristics suggest a common formal pathogenesis. The ultrastructural correlate of DWI+LE appears to be intramyelinic sheath edema. Contrary to stroke, restricted water diffusion in the setting of DWI+LE may be reversible. Reversibility is likely dependent upon the type and severity of insult. DWI+ LE may be an early stage of white matter damage germane to a wide variety of disorders triggered by exogenous or endogenous factors, and its low incidence may reflect its short duration.

FIGURES AND LEGENDS

Figure 1: 17 year-old patient received intrathecal methotrexate for treatment of ALL. Axial images (left to right: DWI, ADC, FLAIR) demonstrate increased DWI signal with corresponding low ADC in the left frontoparietal white matter. Patient made full clinical and imaging recovery

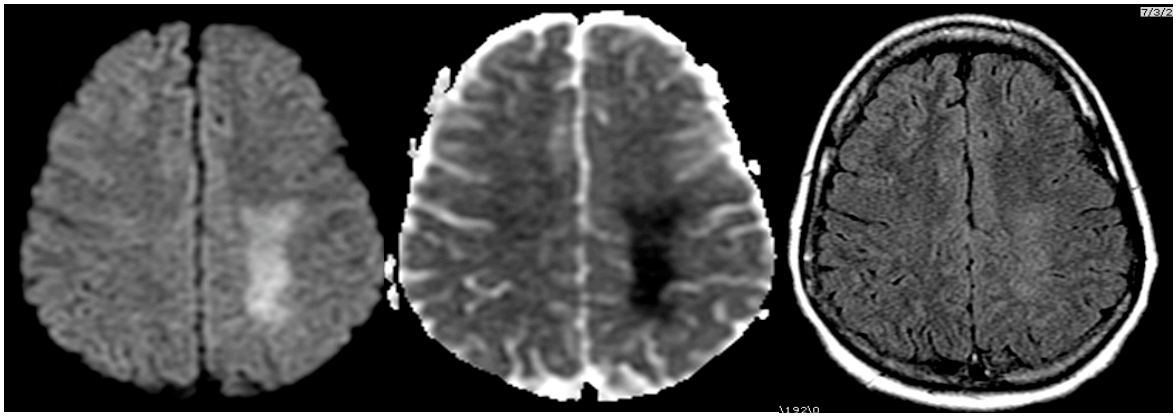

Figure 2: 54 year-old patient presented 18 days following a severe hypoxic event with active use of benzodiazepines, opiates, and cocaine. Images (left to right: DWI, ADC, FLAIR) show increased DWI signal with corresponding low ADC in bilateral subcortical white matter. Patient made remarkable clinical recovery and imaging resolution

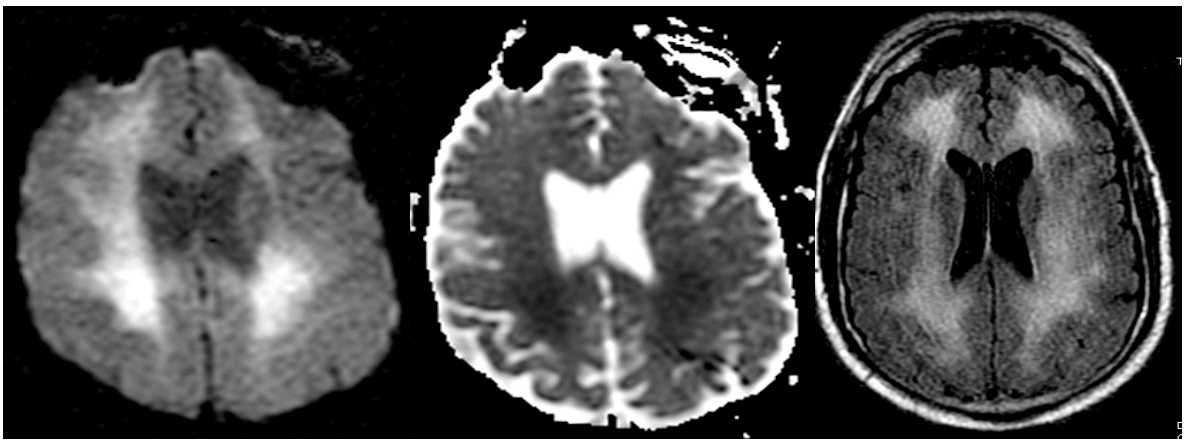

Figure 3: 69 year-old patient presented hypoglycemic with complaints of dizziness. Coronal images (left to right: DWI, ADC, FLAIR) show increased DWI signal with corresponding low ADC in the splenium of the corpus callosum. There was full clinical recovery.

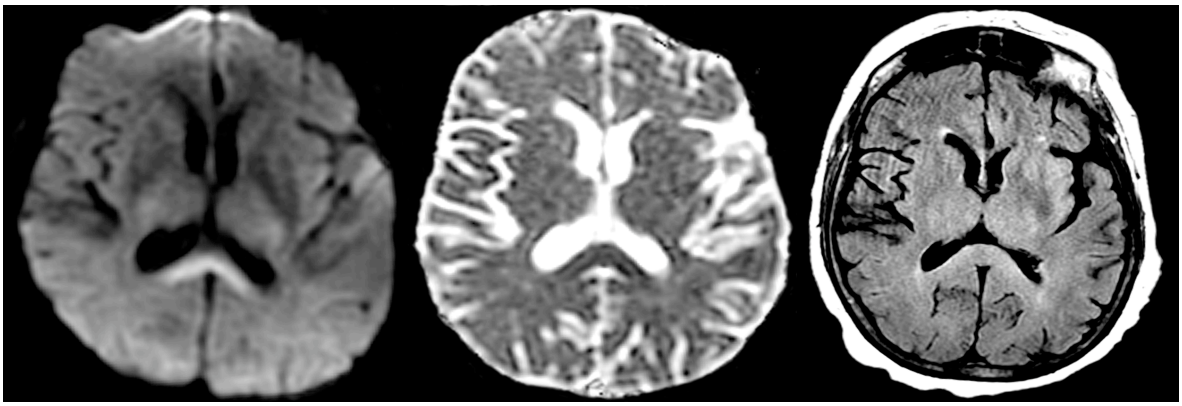

Figure 4: 42 year-old patient on lamictal, topamax, and tripeptal. Images (left to right: axial DWI, ADC, coronal FLAIR) demonstrate increased DWI signal with corresponding low ADC in the splenium of the corpus callosum.

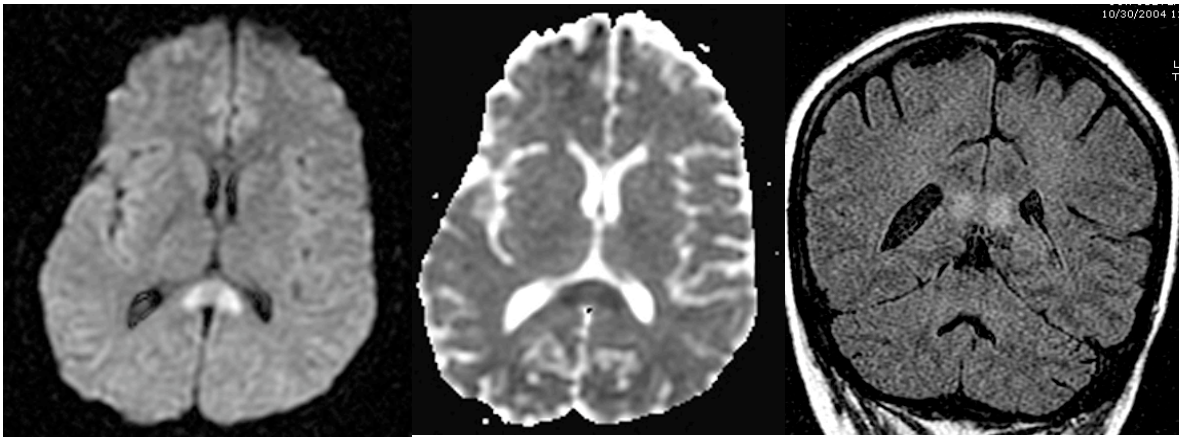

TABLES

TABLE A: TOXIC ETIOLOGY

Clinical Information	Age	DWI	Outcome/Resolution
Intrathecal methotrexate for leukemia	13 years	Bilateral corona radiata and cortical spinal tracts	Symptoms and DWI fully resolved.
Aphasia and mental status change following intrathecal methotrexate for leukemia	17 years	Left frontoparietal white matter	Symptoms and DWI fully resolved.
Mental status change following intrathecal methotrexate for leukemia	16 years	Bilateral frontoparietal white matter	Symptoms and DWI fully resolved.
Intravenous methotrexate for Burkitt's lymphoma	52 years	Right corona radiata	Complete clinical recovery. Imaging unknown.
Altered mental status, gait disturbance and facial droop following attempted aspirin overdose and abrupt cessation of antipsychotics	64 years	Bilateral periventricular white matter	2 weeks later symptoms fully resolved. Imaging unknown.
Myoclonic jerking and syncope at hemodialysis. After extensive work-up deemed primarily heroin-related	53 years	All lobes of the cerebral hemispheres, cerebellum and corpus callosum	Symptoms fully resolved within 8 days. Imaging unknown.
Found unresponsive at psychiatric facility with reports of crack use in his room. Positive urine toxicology for cocaine and opiates.	43 years	Bilateral periventricular white matter and left cerebellum	Died 8 days following admission with no interval clinical improvement.

TABLE B: TRAUMA/HYPOXIC ETIOLOGY

Clinical Information	Age	DWI	Outcome/Resolution
Unstrained back-seat passenger in an auto collision. Glasgow Coma Score of 6 on scene requiring intubation	11 years	Corpus callosum, left pons, right midbrain, left anterior temporal white matter, and left corona radiata	Significant improvement in cognition and speech. Imaging unknown.
Motor vehicle collision with positive loss of consciousness. Glasgow Coma Score of 8 on scene requiring intubation	13 years	Bilateral frontal white matter, deep left parietal white matter and corpus callosum	Cognition slowly improved to near baseline in one week. Imaging unknown.
Non-accidental trauma. Presented to emergency room with agonal breathing requiring intubation.	2 months	Corpus callosum and bilateral optic radiations	Developmental delay and increased tone. Imaging showed partial resolution.
Non-accidental shaking injury and head trauma the day before admission.	2 years	Left cerebral white matter, right inferior frontal lobe, and bilateral thalami	Partial clinical recovery. Imaging unknown.
Motor vehicle collision with change in mental status 8 days following admission.	20 years	Bilateral centrum semiovale, periventricular frontal, parietal, and temporal white matter. Corpus callosum	Significant clinical improvement in cognition and ambulation. Imaging unknown.
Subdural hematoma. Required surgical drainage.	2 months	Entire corpus callosum. Restricted diffusion not seen until six days following surgery	Remarkable clinical recovery upon discharge two weeks later. Imaging unknown.
Subarachnoid hemorrhage	57 years	Entire corpus callosum	Clinical and imaging follow-up not known.

TABLE C: TOXIC/HYPOXIC ETIOLOGY

Clinical Information	Age	DWI	Outcome/Resolution
Found unresponsive by friends. Glasgow Coma Score of 3 in the field. Positive urine toxicology for cocaine and opiates	21 years	Bilateral cerebral and cerebellar hemispheres. Genu and splenium of the corpus callosum	Partial clinical recovery. Alert, oriented and able to following simple commands one month after admission. Imaging unknown
Pulseless electric activity secondary to drug overdose. Documented benzodiazepine and cocaine abuse	31 years	Bilateral posterior limbs of the internal capsule extending to cerebral peduncles	Died 2 days following admission
Pulseless electrical activity secondary to drug overdose. Documented opiate and cocaine abuse	25 years	Bilateral parietal periventricular white matter and cerebellum	Recovered much of speech, sensation, and motor strength 5 months following admission. Imaging unknown
Found by police unable to follow commands and reports of visual changes. Patient had respiratory arrest 18 days prior from a drug overdose. Documented cocaine, benzodiazepine and opiate abuse.	54 years	Bilateral periventricular and subcortical white matter. No abnormality was seen on imaging obtained directly after his respiratory arrest.	Remarkable clinical recovery within one month. DWI showed improvement one month later and complete normalization within 2 months.

TABLE D: NEONATAL HYPOXIC/METABOLIC ETIOLOGY

Clinical Information	Age	DWI	Outcome/Resolution
Delivered via C-section pale, limp, and apneic. Hyponatremia, hypokalemia, hypocalcemia and elevated liver enzymes	4 days	Bilateral periventricular white matter	Neurologic exam one year later showed no change in bilateral increased tone in upper and lower extremities. Imaging unknown.
Vacuum-assisted delivery with hyperkalemia, hyponatemia, and elevated direct bilirubin	3 days	Bilateral posterior periventricular white matter	Clinical and imaging follow-up not known.
Neonatal hypoxia with hypocalcemia and elevated direct bilirubin	6 days	Bilateral periventricular white matter	Clinical and imaging follow-up not known.
Neonatal hypoxia with Hypochloremia, hyopokalemia and elevated liver enzymes	7 days	Bilateral subcortical frontal, parietal, and occipital white matter	Clinical and imaging follow-up not known.

TABLE E: METABOLIC ETIOLOGY

Clinical Information	Age	DWI	Outcome/Resolution
Dizziness with serum glucose of 40	69 years	Splenium of corpus callosum	Symptoms fully resolved. DWI normal 5 months later.
Rapidly corrected hyponatremia. Sodium of 107 corrected to 122 within 24 hours.	77 years	Central midbrain	Clinical and imaging follow-up not known.

TABLE F: SEIZURE/METABOLIC ETIOLOGY

Clinical Information	Age	DWI	Outcome/Resolution
Infant with seizure, hypocalcemia and dehydration	4 months	Bilateral occipital and temporal white matter	Clinical and imaging follow-up not known.
Neonatal seizure with hyponatremia, hypokalemia. Patient has Goldenhar syndrome.	1 day	Posterior corpus callosum	DWI normal 2 years later

TABLE G: ANTIEPILEPTIC ETIOLOGY

Clinical Information	Age	DWI	Outcome/Resolution
Long standing epilepsy admitted on oxcarbazepine and valproic acid	19 years	Splenium of the corpus callosum	Clinical and imaging follow-up not known.
Epilepsy following car crash 20 years ago. Admitted on oxcarbazepine, lamotrigine, and topiramate	42 years	Splenium of the corpus callosum	Clinical and imaging follow-up not known.

TABLE H: HYPOXIC ETIOLOGY

Clinical Information	Age	DWI	Outcome/Resolution
Pulseless electrical activity secondary to aspiration. History of a demyelinating disorder of unclear etiology that was in remission.	27 years	Diffuse confluent white matter involvement	Died 19 days after hypoxic event.

TABLE I: TRAUMA ETIOLOGY

Clinical Information	Age	DWI	Outcome/Resolution
Go-cart accident with head trauma.	14 years	Splenium of the corpus callosum	Clinical and imaging follow-up not known.

TABLE J: UNKNOWN ETIOLOGY

Clinical Information	Age	DWI	Outcome/Resolution
Mental status change and headache. Negative work-up	56 years	Right splenium of corpus callosum	Clinical and imaging follow-up not known
Admitted for seizures with meningitis also with history of AIDS and lymphoma. Likely multi-factorial etiology.	43 years	Splenium of the corpus callosum	Clinically recovered. Imaging shows improvement within 2 weeks and then normalization 2 years later.
Possibly autoimmune encephalitis	22 years	Bilateral external capsules	Clinical and imaging follow-up not known.
Acute onset of right arm paralysis. Urine toxicology negative. History of relapsing-remitting leukoencephalopathy of unknown etiology	29 years	Left parietal and occipital white matter. Splenium of the corpus callosum	Complete resolution of symptoms within 3 days. Imaging not known.

REFERENCES

1) Rabi, I.I., Zacharias, J.R., Millman, S., and Kusch, P. 1938. A new method of measuring nuclear magnetic moment. *Physical Review*. 53:318.

2) Lauterbur, P.C. 1973. Image formation by induced local interactions: examples of employing nuclear magnetic resonance. *Nature*. 242:190–191

3) Damadian, R., Goldsmith, M., Minkoff, L. 1977. NMR in cancer: XVI. Fonar image of the live human body. *Physiological Chemistry and Physics*. 9:97–100.

4) Salibi, N., Brown, M. 1998. *Clinical MR Spectroscopy*. New York. Wiley-Liss.

5) Cardoza, J.D., Herfkens, R.J. 1994. *MRI Survival Guide*. New York. Raven Press.

6) Moritani, T., Ekholm, S., and Westesson, P.L. 2009. *Diffusion-Weighted MR Imaging of the Brain*. London. Spinger.

7) Moseley, M.E., Kucharczyk, J., Mintorovitch, J., Cohen, Y., Kurhanewicz, J., et al. 1990. Diffusion-weighted MR imaging of acute stroke: correlation with T2-weighted and magnetic susceptibility-enhanced MR imaging in cats. *AJNR Am J Neuroradiol* 11:423-429.

8) Mukherji, S.K., Chenevert, T.L., Castillo, M. 2002. Diffusion-weighted magnetic resonance imaging. *J Neuro-Ophthalmol*. 22:118-122.

9) Sevick, R.J., Kanda, F., Mintorovitch, J., Arieff, A.I., Kucharczyk, J., et al. 1992. Cytotoxic brain edema: assessment with diffusion-weighted MR imaging. *Radiology*. 185:687-90.

10) Filley, C.M., Kleinschmidt-DeMasters, B.K. 2001. Toxic leukoencephalopathy. *N Engl J Med*. 345:425-432.

11) Baehring, J.M., and Fulbright, R.K. 2008. Delayed leukoencephalopathy with stroke-like presentation in chemotherapy recipients. *J Neurol Neurosurg Psychiatry*.79:535.

12) Videnovic, A., Semenov, I., Chua-Adajar, R., Baddi, L., Blumenthal, D.T., et al. 2005. Capecitabine-induced multifocal leukoencephalopathy: a report of five cases. *Neurology*. 65:1792–4.

13) Chen, C.Y., Lee, K.W., Lee, C.C., Chung, H.W., and Zimmerman, R.A. 2000. Heroin-induced spongiform leukoencephalopathy value of diffusion MR imaging. *J Comut Assist Tomogr*. 24:735-7.

14) Bega, D.S., McDaniel, L.M., Jhaveri, M.D., Lee, V.H. 2009. Diffusion weighted imaging in heroin-associated spongiform leukoencephalopathy. *Neurocrit Care.*10:352-4.

15) Wolters, E.C., van Wijngaarden G.K., Stam, F.C., Rengelink, H., Lousberg, R.J., et al. 1982. Leukoencephalopathy after inhaling heroin pyrolysate. *Lancet.* 2:1233-7.

16) Okeda, R., Shibutani, M., Matsuo, T., Kuroiwa, T., Shimokawa, R., et al. 1990. Experimental neurotoxicity of 5-fluorouracil and its derivatives is due to poisoning by the monofluorinated organic metabolites, monofluroacetic acid and alpha-fluoro-beta-alanine. *Acta Neuropathol*. 81:66-73.

17) Okeda, R., Karakama, T., Kimura, S., Toizumi, S., Mitsuchima, T., et al. 1984. Neuropathologic study on chronic neurotoxicity of 5-fluorouracil and its masked compounds in dogs. *Acta Neuropathol*. 63:334-43.

18) Ryan, A., Molloy, F., Farrell, M., and Hutchinson, M. 2005. Fatal toxic leukoencephalopathy: clinical, radiological and necropsy findings in two patients. *J neurol neurosurg psychiatry*. 76:1014-16

19) Custodio, C.M., and Basford, J.R. 2004. Delayed postanoxic encephalopathy: a case report and literature review. *Arch Phys Med and Rehabil*. 85:502-5

20) Lee, H., and Lyketsos C. 2004. Delayed Post-Hypoxic Leukoencephalopathy. *Psychosomatics*. 42:530-3

21) Sener, R.N. 2007. Maple syrup urine disease: diffusion MRI, and proton MR spectroscopy findings. *Comput Med Imaging Graph.* 31:106-10.

22) Jan, W., Zimmerman, R.A., Wang, Z.J., Berry, G.T., Kaplan, P.B., et al. 2003. MR diffusion imaging and MR spectroscopy of maple syrup urine disease during acute metabolic decompensation. *Neuroradiology.* 45:393-9.

23) Vermathen, P., Robert-Tissot, L., Pietz, J., Lutz, T., Boesch, C., and Kreis, R. 2007. Characterization of white matter alterations in phenylketonuria by magnetic resonance relaxometry and diffusion tensor imaging. *Magn Reson Med.* 58:1145-56.

24) Kim, S,S., Chang, K.H., Kim, S.T., Suh, D.C., Cheon, J.E., et al. 1999. Focal lesion in the splenium of the corpus callosum in epileptic patients: antiepileptic drug toxicity? *AJNR Am J Neuroradiol.* 20:125-9

25) Prilipko, O., Delavelle, J., Lazeyras, F., and Seeck, M. 2005. Reversible cytotoxic edema in the splenium of the corpus callosum related to antiepileptic treatment: report of two cases and literature review. *Epilepsia.* 46:1633-6.

26) Anneken, K., Evers, S., Mohammadi, S., Schwindt, W., and Deepe, M. 2008. Transient lesion in the splenium related to antiepileptic drug: case report and pathophysiological insights. *Seizure*. 17:654-7.

27) Mahoney, D.H., Shuster, J.J., Nitschke, R., Lauer, S.J., Steuber, C.P., et al. 1998. Acute neurotoxicity in children with B-precursor acute lymphoid leukemia: an association with intermediate-dose intravenous methotrexate and intrathecal triple therapy-- a Pediatric Oncology Group study. *J Clin Oncol.*16:1712-22

28) Li, A.M., Chau, V., Poskitt, K.J., Sargent, M.A., Lupton, B.A., et al. 2009. White matter injury in term newborns with neonatal encephalopathy. *Pediatr Res*. 65:85–9.

29) Auer, R.N. 2004. Hypoglycemic brain damage. *Metab Brain Dis.*19:169-75.

30) Ma, J.H., Kim, Y.J., Yoo, W.J., Ihn, Y.K., Kim, J.Y., et al. 2009. MR imaging of hypoglycemic encephalopathy: lesion distribution and prognosis prediction by diffusion-weighted imaging. *Neuroradiology*. 51:641–9.

31) Ruzel, K., Campeau, N., and Miller, G. 2004. Early diagnosis of central pontine myelinolysis with diffusion-weighted imaging. *Am J Neuroradiology.* 25:210-213.

32) Cohen-Gadol, A.A., Britton, J,W., Jack, C.R. Jr, Friedman, J.A., and Marsh, W.R. 2009. Transient postictal magnetic resonance imaging abnormality of the corpus callosum in a patient with epilepsy. Case report and review of the literature. *J Neurosurg.* 97:714-7.

33) Faden, A.I., Demediuk, P., Panter, S.S., and Vink, R. 1989. The role of excitatory amino acids and NMDA receptors in traumatic brain injury. *Science.* 244:798-800.

34) Arfanakis, K., Haughton, V.M., Carew, J.D., Rogers, B.P., Dempsey, R.J., et al. 2002. Diffusion tensor MR imaging in diffuse axonal injury. *AJNR Am J Neuroradiol.* 23:794-802.

35) Muccio, C.F., De Simone, M., Esposito, G., De Blasio, E., Vittori, C., et al. 2009. Reversible post-traumatic bilateral extensive restricted diffusion of the brain. A case study and review of the literature. *Brain Inj.* 23:466-72.